Microscopic Nature of Ferro- and Antiferromagnetic Interface Coupling of Uncompensated Magnetic Moments in Exchange Bias Systems

M. Gruyters[1,*] and D. Schmitz[2]

[1]*Institut für Physik, Humboldt Universität zu Berlin, Newtonstrasse 15, 12489 Berlin, Germany*
[2]*Hahn-Meitner-Institut Berlin, Glienicker Strasse 100, 14109 Berlin, Germany*

(Received 25 August 2007; published 22 February 2008)

Exchange bias in layered CoO/Fe structures is investigated by x-ray resonant magnetic reflectivity (XRMR) measurements. Element-specific hysteresis loops are obtained from x-ray magnetic circular dichroism effects in the XRMR spectra. Evidence is provided for the existence of different types of uncompensated moments in the antiferromagnetic material. Explanations are given for the microscopic nature of these moments and the complex exchange interactions that determine the magnetization reversal in exchange bias systems.

DOI: 10.1103/PhysRevLett.100.077205 PACS numbers: 75.70.Cn, 75.30.Et, 75.50.Ee

Exchange bias (EB) is one of the most striking phenomena in the magnetism of nanoscaled materials [1]. A shift and a broadening of the hysteresis loop, usually obtained after field cooling, belong to its prominent properties. These effects were discovered more than 50 years ago by Meiklejohn and Bean during the investigation of surface oxidized Co particles [2]. The experimental findings have been explained by exchange coupling between the ferromagnetic (FM) Co core and the antiferromagnetic (AFM) CoO shell. Phenomenologically, the shift and the broadening are attributed to AFM-induced unidirectional and uniaxial anisotropies, respectively.

Uncompensated (UC) magnetic moments associated with the antiferromagnet or its interface were suggested early to mediate the AFM/FM coupling [1,2]. For thin films, it has been shown that a part of these moments rotates when the FM layer is reversed while another part is ''pinned'' in the bias direction by the antiferromagnet [3,4]. Pinned moments lead to a shift of the hysteresis loop along the vertical (magnetization) axis [5,6] as opposed to the shift along the horizontal (field) axis which defines the EB field H_E.

X-ray magnetic circular dichroism (XMCD) provides a powerful method to separate properties of the UC moments from the ones of the ferromagnet. Its high sensitivity and its element specificity allow for quantification of pinned and rotatable UC spins [3] as well as for the detection of vertical loop shifts [4,7]. In the biased state, the preferred coupling of UC moments to the ferromagnet can be parallel (ferromagnetic) [3] or antiparallel (antiferromagnetic) [7]. Despite significant progress, a complete understanding of the microscopic coupling mechanism is still missing and a quantitative model which describes, at least, a certain group of AFM/FM systems has not been reported so far.

Here, we report on EB in a layered CoO/Fe system. The coupling between the AFM and FM materials is systematically varied by inserting nonmagnetic Cu spacers.

The basic layer structure is 40 Å Au/20 Å CoO/x Å Cu/60 Å Fe [6], where a wedge shape allows for the investigation of different Cu thicknesses x of 0, 15, 20, 25, and 30 Å. The magnetic behavior was determined by circular dichroism effects in the x-ray resonant magnetic reflectivity (XRMR) using the helical undulator beam line UE46-PGM at BESSY with a circular polarization of 90%. X-ray reflectivity was measured by a photodiode at an incidence angle of 10° with respect to the surface. Element-specific hysteresis loops were obtained by taking the difference between two magnetic field scans for opposite helicities of the x rays, with the photon energy fixed at selected values of the L_3 edges of Fe (706.5 eV) and Co (776.6 eV) [4]. The XMCD signal, or more precisely, the XRMR asymmetry is defined as the ratio between the reflectivity difference and the reflectivity sum.

The x-ray absorption spectrum (XAS) at the Co L_3 edge detected by total electron yield shows a multiplet structure [Fig. 1(a)] which is characteristic for CoO with the Co ion

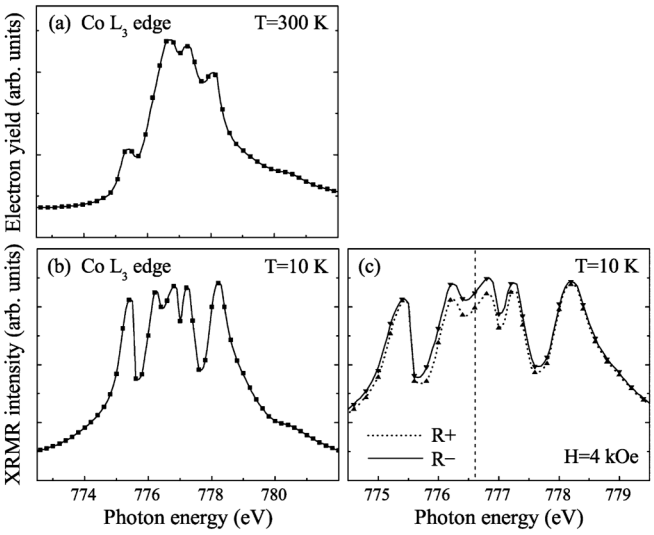

FIG. 1. (a) XAS and (b) XRMR at the Co L_3 edge for a 20 Å CoO/20 Å Cu/60 Å Fe trilayer. (c) XRMR with parallel (R^+) and antiparallel (R^-) alignment of photon helicity and magnetic field direction.

being in a high spin state [8]. The corresponding XRMR spectrum [Fig. 1(b)] reveals a similar peak structure but with different relative intensities and a clear peak at 776.2 eV. Reflectivity is different from electron yield because it depends on both absorptive and dispersive material parameters.

Circular dichroism effects in the XRMR spectrum of CoO in a field of 4 kOe are shown in Fig. 1(c). The resulting Co asymmetry is due to UC moments in the antiferromagnet. It is not due to metallic remnants in the oxidic compound [9], as discussed below.

The XMCD effect in CoO is used to elucidate the behavior of UC moments during magnetization reversal of the FM layer. For CoO/Fe bilayers, both the Fe and the Co loop reveal an appreciable broadening and a negative horizontal shift after field cooling [Figs. 2(a) and 2(b)]. Under certain constraints, the element-specific loops reflect the reversal behavior of the macroscopic CoO and Fe magnetizations. For CoO/Fe bilayers, the main difference in Co and Fe loops is a downward shift for Co which occurs only in the EB state. Vertical shifts in the Fe loops can be discarded because they are either negligible or very small. It can be concluded that a majority of UC Co moments reverses in phase with Fe due to a parallel (ferromagnetic) exchange coupling, whereas a smaller part of the UC Co moments with antiparallel (antiferromagnetic) exchange coupling remains pinned in the bias direction. A similar downward loop shift has recently been found for UC Fe moments in FeF_2/Co bilayers [7].

The spin configuration obtained in maximum positive and negative fields is schematically illustrated by three representative arrows close to the decreasing and increasing field branches of the loops (Fig. 2). Solid and dotted arrows refer to pinned and reversed UC moments, respectively. The direction of the arrows refers to the orientation with respect to the direction of H which agrees with the direction of the Fe saturation magnetization.

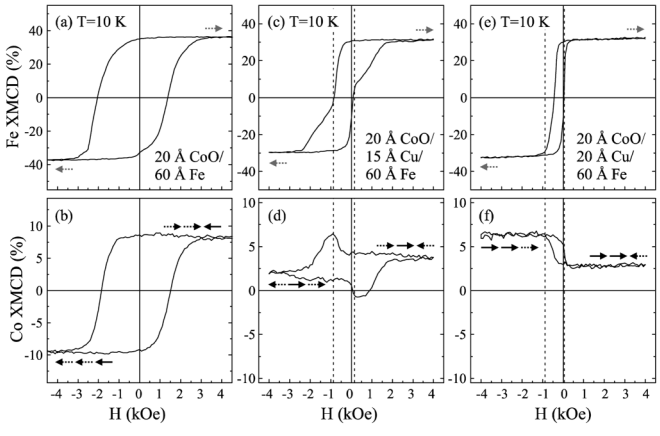

FIG. 2. Fe (top) and Co (bottom) XMCD hysteresis loops for 20 Å CoO/x Å Cu/60 Å Fe trilayers with increasing Cu spacer thickness: $x = 0$ (a),(b), $x = 15$ (c),(d), and $x = 20$ (e),(f). At $T = 10$ K after cooling in $H^{\mathrm{COOL}} = +2.5$ kOe from $T = 300$ K.

The loop behavior of UC moments changes by inserting nonmagnetic spacers between the AFM and FM materials. Instead of a decrease, an increase in XMCD signal occurs on the negative field side for 20 Å Cu [Fig. 2(f)]. The loop behavior is explained by pinning of a larger part of UC moments with FM coupling ($\approx 75\%$) and reversal of a smaller part of UC moments with AFM coupling ($\approx 25\%$). The behavior is essentially opposite to $x = 0$. This is illustrated by the arrows which describe the overall behavior and do not provide a quantitative description.

For decreasing fields down to $H = -1$ kOe, the Co reversal for $x = 15$ [Fig. 2(d)] is basically the same as for $x = 20$. With further decreasing fields, a part of the UC moments with FM exchange coupling reverses in the direction of H for $x = 15$. Some UC moments virtually follow the Fe magnetization for $H < -1$ kOe.

We explain the dependence on Cu spacer thickness by different microscopic mechanisms for FM and AFM exchange coupling. For zero and small Cu thicknesses, FM coupling dominates the loop behavior which is likely to be due to a short-range direct exchange between Co atoms in the CoO and Fe at the immediate CoO/Fe interface. For larger Cu thicknesses, the influence of AFM coupling significantly increases indicating that a long-range indirect exchange dominates the reversal behavior. The remaining FM coupling component is also long range, but the corresponding UC moments are almost completely pinned. The behavior for $x = 15$ represents an intermediate case between $x = 0$ and $x = 20$, possibly due to pinholes in the spacer which locally maintain CoO/Fe interfaces.

Long-range indirect exchange across nonmagnetic spacers has been intensively studied in FM/metal/FM layers. In many systems, exchange coupling has been found to oscillate between parallel and antiparallel as a function of spacer thickness. This behavior has been explained by a Ruderman-Kittel-Yoshida-Kasuya (RKKY) interaction which is based on spin polarization of the conduction electrons of the nonmagnetic spacer. The latter is also likely to apply for the CoO/Cu/Fe system but without obvious oscillations in the magnetic properties. Two effects may explain the nonoscillatory behavior. With respect to the atomic spatial distribution, the spin configuration at a CoO/Cu interface with localized Co moments differs from the delocalized spin density at a completely metallic FM/metal interface. A superposition of contributions from different types of Co moments in the near-interface region therefore strongly affects the interlayer coupling. Alternatively, the specific type of conduction electrons which mediate the coupling may play the decisive role. If mainly d electrons are involved, electron-electron interactions can lead to strong damping or even to disappearance of the oscillatory behavior [10].

Further insight into the coupling mechanisms is gained from the temperature dependence [Fig. 3]. It can be divided into two regimes, above and below 190 K. In the lower T regime [Figs. 3(a)–3(d)], the response to external fields increases with increasing temperature but the configuration

of the UC moments remains similar to the initial one at 10 K. Deviations occur due to a weakening of the magnetic interactions at the CoO/Fe interface and within the CoO. A drastic change in the loop behavior appears at $T = 190$ K. In the higher T regime [Figs. 3(f) and 3(g)], UC moments are not pinned as evidenced by the missing vertical loop shift. At 220 K, exchange interaction between the two different types of UC moments leads to an antiparallel alignment which is no longer present at 250 K. At $T = 10$ K, the preferred antiparallel alignment between the two types of UC moments is hindered on the negative field side [Fig. 3(a)] which leads to a contribution to the unidirectional anisotropy.

We conclude that a freezing process occurs between about 190 and 220 K which determines the reversal behavior and the spin configuration of CoO at low temperatures. With decreasing temperature, the process starts with interaction among UC moments followed by pinning of the UC moments with FM exchange coupling.

Our interpretation of the hysteresis loops is valid only under the assumption of same signs between the XMCD signals and the magnetic moments for both elements. Because of momentum transfer and interference effects in XRMR [11], the sign (parallel or antiparallel) of the exchange coupling cannot be inferred by simply inspecting the Fe and Co hysteresis loops. In our work, the correct sign of the XMCD signals in the XRMR mode is determined by comparison of XMCD effects in energy spectra across the L_3 and L_2 edges recorded by two methods, electron yield and reflectivity. Above the spin freezing temperature $T_F \approx 200$–220 K of CoO, Fe and Co moments show parallel orientations in both detection modes. This is valid for all investigated Cu spacer thicknesses. The correct assignment is confirmed by hysteresis loops recorded by magnetometry [6] which also imply parallel orientations of both moments throughout the whole magnetization reversal at temperatures above T_F. It is thus ensured that, in our experiments, any relative change in sign or strength of the XMCD signals (in dependence on temperature and spacer thickness) originates from real changes in the magnetic properties and not from subtle features of the scattering process.

At $T = 190$ K, the Co loop is strongly curved for $x = 20$ [Figs. 3(e) and 4(d)]. The reversal extends over a large field range and is not completed in the decreasing field branch by the maximum field of -4 kOe. There is no obvious correlation to the corresponding Fe loop [Fig. 4(c)]. Contrary to this, a strong correlation between Co and Fe loop is present for $x = 15$ [Figs. 4(a) and 4(b)] which supports the conclusion that FM exchange coupling is strongly reduced with increasing spacer thickness. For strong FM coupling, UC moments follow the Fe magnetization as in the case of $x = 15$ and certainly of $x = 0$. For $x = 20$, other coupling effects dominate.

The complex behavior in dependence on temperature and spacer thickness [Figs. 1–4] can be explained in the framework of a model recently suggested for the magnetic coupling of granular CoO layers [9,12]. Different types of Co moments exist in the CoO. The majority of Co atoms (Co_{AFM}) takes part in a common AFM interaction being characteristic for bulk CoO. Additionally, there are Co atoms (Co_{UC}) leading to UC moments. For the former, the magnetic behavior is dominated by common superexchange between Co ions via intervening oxygen ions. The latter are involved in the AFM order, but they are also responsible for the coupling to the Fe moments (Fe_{FM}) and, therefore, for EB. Considering this and the fact that two types of UC moments with parallel (P) and antiparallel (AP) coupling exist, the microscopic exchange interactions J involved in the CoO/Fe coupling can be summarized as follows: $J(Fe_{FM} - Co^{P}_{UC})$, $J(Fe_{FM} - Co^{AP}_{UC})$, $J(Co^{P}_{UC} - Co_{AFM})$, $J(Co^{AP}_{UC} - Co_{AFM})$, and $J(Co^{P}_{UC} - Co^{AP}_{UC})$.

In addition to the exchange interactions J, the magnetic anisotropy K of the antiferromagnet plays a decisive role for EB [9,12]. The anisotropy energy $K(Co_{AFM})$ and the exchange energy $J(Co_{UC} - Co_{AFM})$ provide the pinning of the UC moments at lower temperatures. The underlying physical picture is best described by UC moments which are embedded in an antiferromagnetic matrix of Co_{AFM} atoms [9,12]. Field cooling from above the AFM ordering

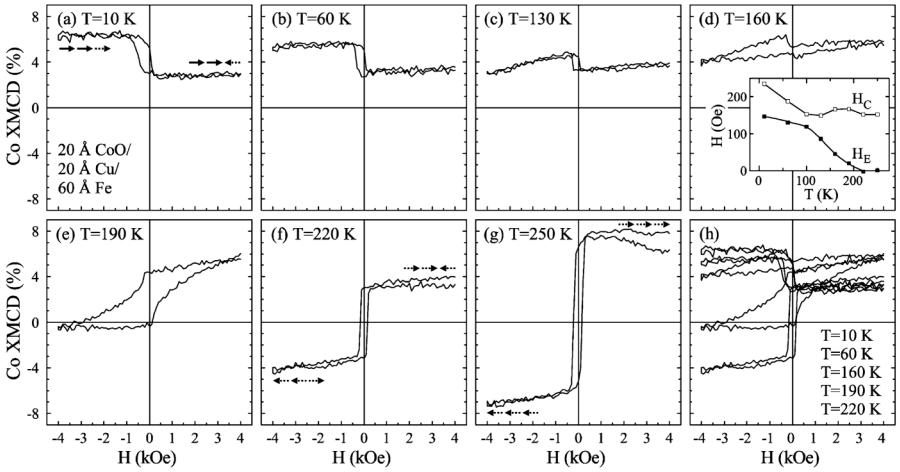

FIG. 3. Co XMCD hysteresis loops for a 20 Å CoO/20 Å Cu/60 Å Fe trilayer with increasing temperature after field cooling in +2.5 kOe to $T = 10$ K. The inset shows the corresponding loop shift H_E and half-width H_C determined by the Fe loops.

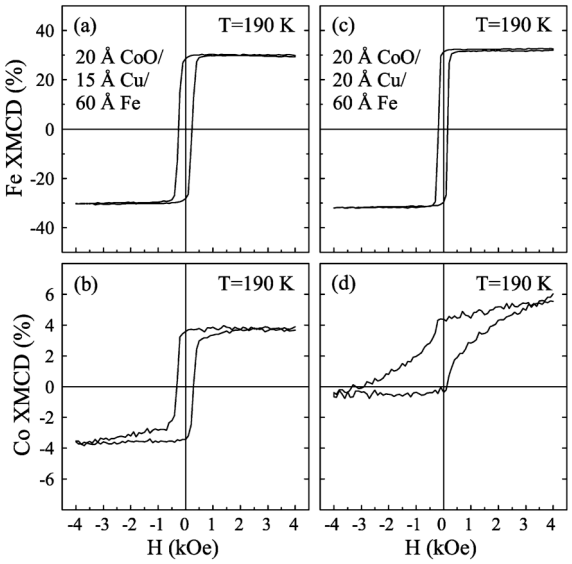

FIG. 4. Same as Figs. 2(c)–2(f) after increasing the temperature to $T = 190$ K.

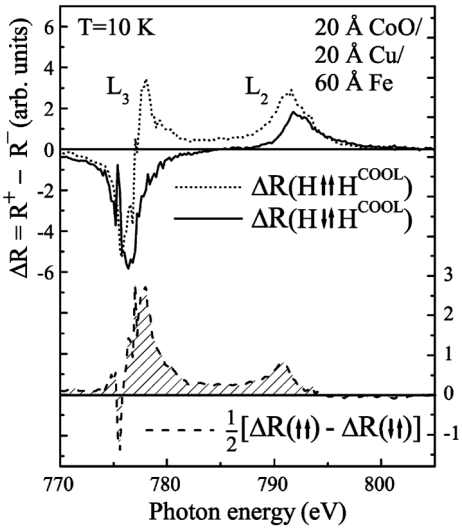

FIG. 5. XMCD effect at the Co L edges for a 20 Å CoO/20 Å Cu/60 Å Fe trilayer after field cooling to 10 K: Difference ΔR of XRMR spectra with parallel (R^+) and antiparallel (R^-) alignment of photon helicity and magnetic field direction.

temperature leads to freezing into a spin configuration that accommodates to the orientation of $K(\mathrm{Co_{AFM}})$ and to the orientation of the UC moments.

The external field affects the spin configuration of the frozen antiferromagnetic matrix through reversal of UC moments. The large loop broadening for $x = 20$ at $T = 190$ K [Fig. 4(d)] and for $x = 0$ at $T = 10$ K [Figs. 2(a) and 2(b)] originates from reversal of UC moments with FM coupling. In addition to unidirectional anisotropy, $\mathrm{Co}^P_{\mathrm{UC}}$ moments thus induce higher-order anisotropies, in the simplest case an uniaxial anisotropy [12].

For $x = 20$, $\mathrm{Co}^P_{\mathrm{UC}}$ moments are pinned at $T = 10$ K because the exchange coupling to Fe, $J(\mathrm{Fe_{FM}} - \mathrm{Co}^P_{\mathrm{UC}})$, is not sufficient to overcome the energy barrier given by the coupling to the antiferromagnetic matrix, $J(\mathrm{Co}^P_{\mathrm{UC}} - \mathrm{Co_{AFM}})$ and $K(\mathrm{Co_{AFM}})$, respectively.

Different properties of $\mathrm{Co}^P_{\mathrm{UC}}$ and $\mathrm{Co}^{AP}_{\mathrm{UC}}$ moments are apparent from the dichroism signal $\Delta R = R^+ - R^-$ in the XRMR spectra (Fig. 5). According to the Co loop behavior for $x = 20$ and $T = 10$ K [Fig. 3(a)], ΔR corresponds to the sum (difference) spectrum of $\mathrm{Co}^P_{\mathrm{UC}}$ and $\mathrm{Co}^{AP}_{\mathrm{UC}}$ for H being antiparallel (parallel) to H^{COOL}. The difference $\frac{1}{2}[\Delta R(\uparrow\uparrow) - \Delta R(\downarrow\uparrow)]$ at the bottom of Fig. 5 is therefore mainly due to $\mathrm{Co}^{AP}_{\mathrm{UC}}$. The relative intensity and the same sign of the two peaks in this spectrum indicate differences in the properties of the two types of UC moments which are likely to be related to the different coupling strength to the AFM CoO. A quantitative analysis is difficult, one reason being that dichroism effects in XRMR are not exclusively due to absorption.

Finally, we focus on new insights from our work which have important implications for a microscopic understanding of exchange bias and future theoretical modeling: (A) Exchange bias in layered systems with CoO is determined by two different types of UC moments with FM and AFM exchange coupling. (B) The interaction between Fe and UC moments with AFM coupling is mainly indirect. (C) UC moments with FM coupling account for unidirectional plus higher-order anisotropies. (D) UC moments with AFM coupling are characterized by weak coupling to the AFM CoO. (E) There are exchange interactions among UC moments which contribute to unidirectional anisotropy. (F) The spin configuration in CoO at low temperatures is established by a freezing process at $T_F \approx$ 200–220 K [6].

Support by N. Darowski and E. Schierle during the beam time is gratefully acknowledged.

*Corresponding author.
markus.gruyters@gmx.de

[1] J. Nogués and I. K. Schuller, J. Magn. Magn. Mater. **192**, 203 (1999).
[2] W. H. Meiklejohn and C. P. Bean, Phys. Rev. **105**, 904 (1957).
[3] W. J. Antel, F. Perjeru, and G. R. Harp, Phys. Rev. Lett. **83**, 1439 (1999).
[4] H. Ohldag *et al.*, Phys. Rev. Lett. **91**, 017203 (2003).
[5] J. Nogués, C. Leighton, and I. K. Schuller, Phys. Rev. B **61**, 1315 (2000).
[6] M. Gruyters, Phys. Rev. Lett. **95**, 077204 (2005).
[7] H. Ohldag, H. Shi, E. Arenholz, J. Stöhr, and D. Lederman, Phys. Rev. Lett. **96**, 027203 (2006).
[8] J. H. Park, S. W. Cheong, and C. T. Chen, Phys. Rev. B **55**, 11 072 (1997).
[9] M. Gruyters, Europhys. Lett. **77**, 57 006 (2007).
[10] Y. Takahashi, Phys. Rev. B **56**, 8175 (1997).
[11] S. Roy *et al.*, Phys. Rev. Lett. **95**, 047201 (2005).
[12] M. Gruyters, J. Magn. Magn. Mater. **320**, 407 (2008); Phys. Rev. B **73**, 014404 (2006).